JOURNAL OF THE FACULTY OF FORESTRY ISTANBUL UNIVERSITY
İSTANBUL ÜNİVERSİTESİ ORMAN FAKÜLTESİ DERGİSİ
ISSN: 0535-8418 e-ISSN: 1309-6257
Online available at / Çevrimiçi erişim Research Article / Araştırma Makalesi
http://dergipark.ulakbim.gov.tr/jffiu - http://dx.doi.org/10.17099/jffiu.01280

Incorporation of hyperspectral imagery and texture information in a SVM method for classifying urban area of southern regions of Tehran, Iran

Ahmad Maleknezhad Yazdi [*] [1], Vahid Eisavi [1], Ali Shahsavari [2]

[1] Tarbiat Modares University, Remote Sensing and GIS Department, M.Sc. in Remote Sensing, Tehran, Iran
[2] Tehran University, Remote Sensing and GIS Department, M.Sc. in Remote Sensing, Tehran, Iran

[*] **Corresponding author e-mail (İletişim yazarı e-posta):** a.malekny@gmail.com

Received (Geliş tarihi): 09.02.2015 **Revised (Düzeltme tarihi):** 19.02.2015 **Accepted (Kabul tarihi):** 19.02.2015

Abstract: Due to rapid population growth over recent decades, changes of urban areas have significantly impacted the environment. Urban is a heterogeneous and highly fragmented environment which has made them a challenging area for remote sensing imagery. The reliability of the information delivered by remote sensing applications in urban area highly depends on the quality of spatial and spectral data. Accordingly, the objective of this study is to analyze the impact of incorporation of Hyperion imagery and textural characteristics of high resolution panchromatic ALI imagery in classifying of urban region of south west of Tehran. To this end, we extracted textural information from panchromatic ALI imagery using gray-level co-occurrence matrix (GLCM) method. Classification was carried out by SVM method in five scenarios: Classification of spectral band of CNT method, classification of spectral bands plus texture with window size 3, size 5, size 7 and size 9. The classification results show that the urban areas of south west of Tehran are insufficiently characterized by the Hyperion satellite imagery. A quantitative assessment of the results demonstrated that the use of texture information improved urban land covers classification. As a result, combining of texture information with Hyperion imagery decreases class confusion specifically in heterogonous classes. The GLCM features show great potential for land use cover classification in heterogeneous areas with rich textural information.

Keywords: Hyperspectral imagery, image texture, GLCM, remote sensing, SVM classification

İran Tahran şehri güney bölgesinde kent alanlarının sınıflandırılmasında SVM yöntemi ile hiperspektral görüntü ve tekstür bilgilerinin birlikte kullanılması

Özet: Son yıllarda hızlı nüfus artışı ve kentsel alanlardaki değişimler çevreyi önemli bir şekilde etkilemiştir. Kentsel alanlar heterojenik ve parçalanmış bir yapıya sahiptir, bu durum uzaktan algılama görüntüleri açısından zorlu bir durum yaratmaktadır. Kentsel alanlarda uzaktan algılama uygulamalarından elde edilen bilgilerin güvenilirliği mekansal ve spektral verilerin kalitesine bağlı olarak değişmektedir. Dolayısıyla, bu çalışmanın amacı Tahran'ın güney batısındaki kentsel bölgede Hyperion görüntüleri ve yüksek çözünürlüklü pankromatik ALI görüntülerinin dokusal özelliklerinin esas etkisini analiz etmektir. Bu amaçla, gri-seviyeli eş-oluşum matrisi (gray-level co-occurrence matrix) (GLCM) yöntemini kullanarak pankromatik ALI görüntülerinden yapısal bilgi ayıklanmıştır. Sınıflandırma beş senaryo halinde SVM yöntemi ile gerçekleştirilmiştir. CNT yöntemiyle spektral bantların sınıflandırılması, spektral bant sınıflandırılması pencere boyutu 3, boyut 5, boyut 7 ve boyut 9. sınıflandırma sonuçları Tahran güney batı kentsel alanların Hyperion uydu görüntüleri ile yeterince karakterize edilemediğini göstermektedir. Sonuçlar yapısal bilgilerin kullanımı ile kentsel arazi sınıflandırmalarının daha başarılı bir şekilde yapılabildiğini göstermektedir. Sonuç olarak, Hyperion görüntüleri ile yapısal bilgilerinin birleştirilmesi heterojenik sınıflandırmada karışıklığı azaltmaktadır. GLCM özellikleri içerdikleri zengin yapısal bilgi ile heterojen alanlarda arazi kullanım sınıflandırmaları için büyük bir potansiyel gösterirler.

Anahtar Kelimeler: Hiperspektral görüntü, görüntü tekstürü, GLCM, uzaktan algılama, SVM sınıflandırması

To cite this article (Atıf): Yazdi, A.M., Eisavi, V., Shahsavari, A., 2016. Incorporation of hyperspectral imagery and texture information in a SVM method for classifying urban area of southern regions of Tehran, Iran. *Journal of the Faculty of Forestry Istanbul University* 66(1): 90-103. DOI: 10.17099/jffiu.01280

1.INTRODUCTION

Due to rapid population growth over recent decades, changes of urban areas have significantly impacted the environment (Pacifici et al., 2009). Although, urban areas represent a small percentage of the global land uses, their monitoring is necessary for evaluation of the human footprint on the environment. Remote sensing data classification is the most common approach for urban land use mapping (Forster, 1985; Ridd, 1995; Carlson and Azofeifa, 1999).

Urban is a heterogeneous and highly fragmented environment which their broad variations in components, constructive materials such as concrete, asphalt, soil, metal, glass and vegetation (Carleer and Wolff, 2006) have made them a complex area for remote sensing resulted in difficulties in detection of their land covers (Ridd, 1995; Small, 2001; Small, 2005). As a result, modeling of these land covers in multispectral imagery with limited spectral bands is a complex process and accompanies with great degrees of inaccuracy.

Hyperspectral imaging with more than ten or hundreds of spectral bands has provided new opportunities for analyzing a variety of materials (Goetz, 2009; Yuntao et al., 2012) which can deal with the deficiency of multispectral sensors. One of these detectors is Hyperion with 224 spectral bands. This detector has been used in some cases for urban studies (Bokoye, 2004; Kateskasem, 2005; Welikanna, 2008; Cavalli et al., 2008). The reliability of the information delivered by remote sensing applications in urban area highly depends on the quality of spatial and spectral data. The identification of relatively small objects, e.g., narrow streets, trees and houses is important in classification of remote sensing data of urban areas (Fauvel et al., 2008). Therefore, besides the hyperspectral imagery, high spatial resolution of imagery is necessary for accurate land use mapping of such a complex scenes. Meanwhile, Hyperion has relatively low spatial resolution (30 m) which is inconvenient for common urban studies. Taking into account of these reasons, it is essential to extract additional information from panchromatic images in order to recognize objects within the scenes, such as texture (Pacifici et al, 2009). In most remote sensing literature, texture information improved the per-pixel classification accuracy (Zhang et al., 2003; Puissant et al., 2005; Pacifici et al., 2009; Murray et al., 2010). However, the impacts of ALI imagery on the classification Hyperion have not been investigated.

One of the abilities of EO-1 satellite, carrying Hyperion detector, is producing a panchromatic image by ALI detector (10 m) at the same time of taking Hyperion imagery. Therefore, this condition makes it possible to apply both sensors at the same time.

The objective of this study is to analyze the impact of incorporation of Hyperion imagery and textural characteristics of high resolution panchromatic ALI imagery in classifying of an urban region. To this end, we extract textural information from panchromatic ALI imagery using gray-level co-occurrence matrix (GLCM) method (Haralick et al., 1973; Haralick, 1979). It was demonstrated that textural features derived from GLCM are the most useful features for improvement of land cover classification accuracy (Shanmugan et al., 1981; Clausi and Yue, 2004). Further, support vector machine (SVM) is used to classify the spectral-structural features after dimensional reduction. Support Vector Machines have shown to be a valid alternative for classifying hyperspectral remote sensing imageries (Melgan and Bruzzone, 2004; Camps and Bruzzone, 2005; Fauvel, 2007).

2.MATERIALS AND METHODS

2.1 Study Area and Data

The study area is located in south west of Tehran, Iran. Tehran features a semi-arid climate. The dominant landcover types in the region include the built-up areas, bare lands, farmlands and orchards. This region contains as much as 1938 hectare of agricultural and residential areas of Tehran and placed adjacent to Azadegan and Persian Gulf highways (Figure / Şekil 1).

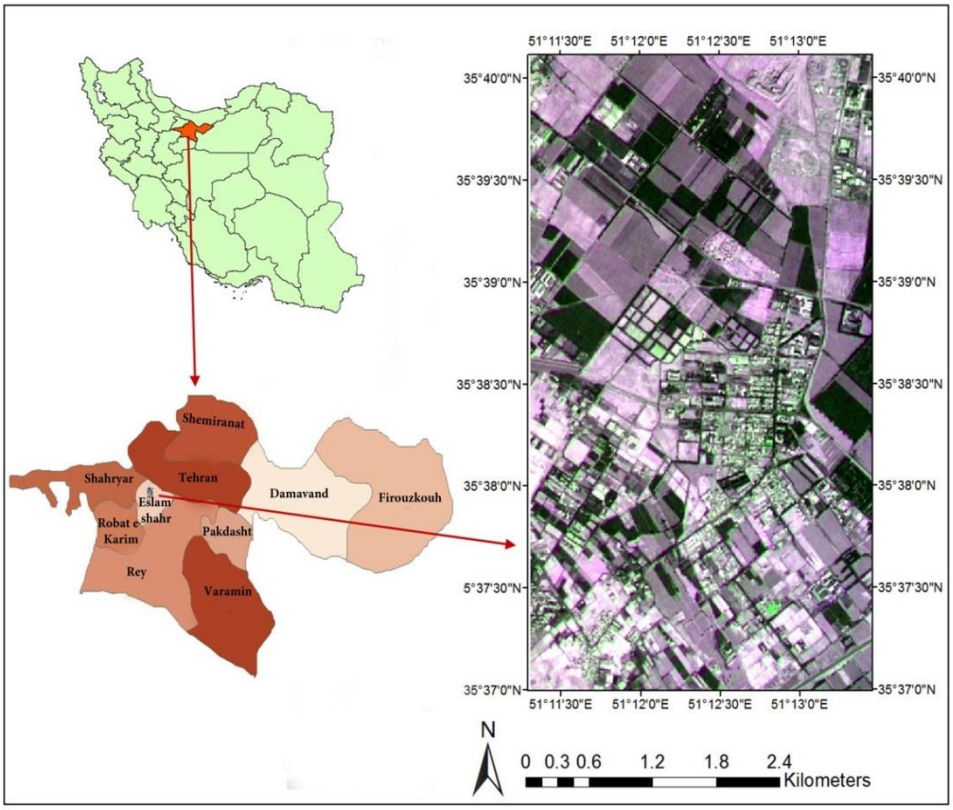

Figure 1. Location of the study area
Şekil 1. Çalışma alanının konumu

Both of images used in this research were taken by EO-1 Satellite. Table / Tablo 1 represents the different characteristics of sensors and images taken by them in detail.

Table 1. Sensors characteristics launched on EO-1 Satellite
Tablo 1. EO-1 uydusu üzerindeki sensör özellikleri

Parameter	ALI Sensor	Hyperion Sensor
Spectral Range	400-2400 nm Multispectral 480-690 nm Panchromatic	400-2500 nm
Spatial Resolution	30 meters	30 Meters
Spectral Resolution	Variable	10 nm
Swath Width	37 km	7.6 km
Panchromatic Spatial Resolution	10 meters	N/A
Number of Bands	10	220
Acquisition Date	10/30/2009	10/30/2009

2.2 Research Methodology

Figure / Şekil 2 illustrates the overall method used in this research.

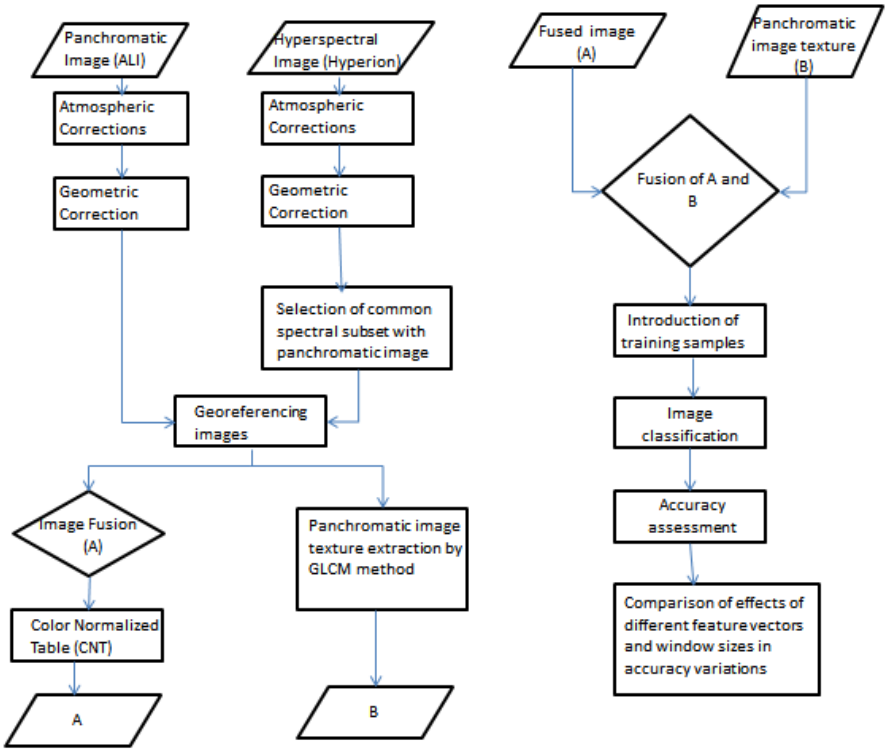

Figure 2. Research methodology
Şekil 2. Araştırma metodolojisi

Hyperspectral images are more vulnerable to the atmospheric effects due to their narrow spectral bandwidth. As a result, implementation of atmospheric correction algorithms are necessary to minimize these effects but prior to this step, striping in hyperspectral images have to be dealt with in order to recover the damaged bands (Kawishwar, 2007).

After removing absorption, non-calibrated and collapsed bands from the initial set of hyperspectral image bands, 220 primary bands diminished to 134 bands. In the next step, FLAASH (Fast Line of Sight Atmospheric Analysis Spectral Hypercubes) algorithm was used for the atmospheric correction. The required solar and meteorological parameters for atmospheric correction are summarized in Table / Tablo 2.

Table 2. Required parameters for atmospheric correction
Tablo 2. Atmosferik düzeltme için gerekli parametreler

Sun Elevation Angle: 8.21 degree	Flight Time: 6:58:50
Sun Azimuth Angle: 112.2 degree	Scene Center Location: Lat: 35.63 Lon: 51.21 degree
Sensor Height: 705 kilometer	Visibility: 40 kilometer
Mean Ground Elevation: 1.1 kilometer	Temperature: 18.1 centigrade

Geometric correction was carried out for geo-referencing images in a high accuracy manner. To achieve this accuracy, the panchromatic image was selected as the base image and geo-referencing was done by 19 ground control points (GCP) and polynomial equations of degree 2 in all regions of the image. Accordingly, we achieved the accuracy of less than half a pixel (0.42 m). Nearest neighborhood method was selected for the image interpolation. In addition, the Hyperion imagery was co-registered for the panchromatic ALI imagery.

The fusion method used in this study is Color Normalized Transformation (CNT), which is based on color components. It exploits the panchromatic image in a direct relationship and is more suitable for images with high correlations. The equation for fusion is:

$$MS_{FK}^{H} = \frac{SMS_K * Pan}{\sum_k^n MS} \quad (1)$$

Where SMS_K DN represents the pixel in kth band and $\sum_k^n MS$ represents the summation of DNs of that pixel in all bands. This operation resulted in 23 bands covering 480 -690 nm spectral range with spectral resolution of 10 nm.

2.3 Texture Extraction

Methods available for extraction of Image texture can be divided into 4 main categories: structural, statistical, model-based and transformation-based. The GLCM is the first method in this field which was introduced by Haralick (1973). This statistical method works on the basis of two parameters: the distance and angle between two pixels in a window by specific size. Texture parameters which called feature vectors are calculated in the next step. Haralick (1973) introduced 23 feature vectors in his first article but later in 1979, he reduced them to 8. In our research, the correlation feature vector was omitted due to some inconsistent values (infinite) and the other ones were investigated which are indicated in Table / Tablo 3.

Table 3. The feature vectors used in the study
Tablo 3. Çalışmada kullanılan vektör özellikleri

$$\mu_i = \sum_{i=0}^{N-1}\sum_{j=0}^{N-1} i p_d(i,j) \quad (2)$$

$$\sigma_i^{\,2} = \sum_{i=0}^{N-1}\sum_{j=0}^{N-1} p_d(i,j)(i-\mu_i)^2 \quad (3)$$

$$\sigma j^{\,2} = \sum_{i=0}^{N-1}\sum_{j=0}^{N-1} p_d(i,j)(j-\mu_i)^2$$

$$\text{Homogeneity} = \sum_i^{N-1}\sum_j^{N-1} \frac{Pd(i,j)}{1+(i-j)^2} \quad (4)$$

$$\text{Contrast} = \sum_i^{N-1}\sum_j^{N-1} P_d(i,j)(i-j)^2 \quad (5)$$

$$\text{Dissimilarity} = \sum_i^{N-1}\sum_j^{N-1} P_d(i,j).|i-j| \quad (6)$$

$$\text{Enthropy} = -\sum_i^{N-1}\sum_j^{N-1} P_d(i,j).\log P_d(i,j) \quad (7)$$

$$\text{Angular Second Moment} = \sum_i^{N-1}\sum_j^{N-1} P_d(i-j)^2 \quad (8)$$

The window size and distance between pixels are two effective parameters in derivation of texture. Variations of these parameters can have considerable effects on the extraction of texture in different land covers. The most optimal distance between pixels in previous work were determined as d=(1,1) (one horizontal distance and one distance in vertical direction) (Hall-Bayer, 2007). Here, this distance was selected as the default distance and window sizes of 3, 5, 7 and 9 were examined for different land covers to reach the most suitable window sizes associated with each land cover. Larger window sizes may lead to loss of some valuable texture measures, such as the dividing edges between different land covers, which plays important roles in the differentiation of them.

2.4 Image Classification

In order to classify land covers, 14 main classes in image area were selected through field surveying and the satellite image with high spatial resolution. Vector zones were also chosen as the reference for training samples in supervised classification (i.e. SVM). These classes along with number of training samples are listed in Table / Tablo 4.

Table 4. Extracted classes from training samples and images
Tablo 4. Üzerinde çalışma yapılan örnekler ve görüntüler

Class number	Number of training samples	Class name	Class number	Number of training samples	Class name
1	342	Corn Fields	8	42	Roads
2	192	Barren Lands	9	57	Tree Row
3	133	Barren Lands Containing Garbages	10	41	Gardens Containing Fruitless Trees
4	126	Fallow Lands	11	170	Ploughed Lands
5	51	Orchards	12	109	Scattered Industries
6	69	Land Without Vegetation Cover	13	47	Warehouses
7	275	Residential Area	14	103	Concentrated Industries

Training and test samples were chosen on basis of stratified random sampling. The proportion governing over division of samples was 4:1. i.e., 20% of samples were used for training classifier and the others were used for validating it (Gualtieri, 2009).

In order to evaluate the efficiency of the GLCM features derived from panchromatic ALI imagery in improvement of land cover classification accuracy, we defined five scenarios as follow: 1) classification of spectral band of CNT method 2) classification of spectral bands plus texture with window size 3 (W3) 3) classification of spectral bands plus texture with window size 5 (W5) 4) classification of spectral bands plus texture with window size 7 (W7) and 5) classification of spectral bands plus texture with window size 9 (W9).

2.5 SVM Method

Classification was carried out by the SVM method. This method was chosen because of the limitation of training samples and its non-parametric nature that enables us to classify texture and spectral information simultaneously. SVM has proven its superiority over common methods such as neural networks and maximum likelihood in previous studies (Féret and Asner, 2013; Mountrakis et al., 2011). SVM in its basic form deals with the problem of the best separator between two classes and tries to find a hyperplane thereby the following optimization equation can be solved:

$$\min\left\{\frac{1}{2}\|w\|^2+C\sum_{i=1}^{k}\xi_i\right\} \qquad (9) \qquad\qquad y_i(w.x_i+b)\geq 1-\xi_i \quad i=1,\ldots,k \qquad (10)$$

Where the minimization of the first part ($\frac{1}{2}\|w\|^2$) leads to the maximization of margins between support vectors. *C* in the second part of eq.2 is used to fine misclassified training samples. However, the unreasonable rise of this parameter results in the reduction of generalization ability of classifier and unfitting with the features available on the image (Mather and Tso, 2009; Goumehei, 2010; Oommen et al., 2008).

The classes in their primary space are generally inseparable and they are projected to a kernel feature space with higher dimensions (Colgan et al., 2012). There are numerous kernels which the associated equations concerning linear, polynomial, radial-basis function (RBF) and sigmoid kernels have been presented in equations 10 to 13.

$$K(x_i,x_j)=x_i^T x_j \qquad (10)$$

$$K(x_i,x_j)=(\gamma x_i^T x_j+r)^d \quad ,\gamma> \qquad (11)$$

$$K(x_i,x_j)= \exp\left(-\gamma\left\|x_i-x_j\right\|^2\right) \ , \gamma> \quad (12)$$

$$K(x_i,x_j)=\tanh(\gamma x_i^T x_j+r) \quad (13)$$

In above equations, *r*, γ and *d* are parameters which are defined manually. Cost parameter (C) which described in prior parts must also be taken into consideration.

In this research, radial basis function kernel was used for classification. The reason behind this selection is its better performance in previous studies (Colgan et al., 2012; Huang et al., 2002; Petropoulos et al., 2010). Moreover, this kernel needs less parameter for tuning compared to the other ones (2 parameters (cost and sigma) compared to 4 parameters in polynomial and 3 in sigmoid kernels).

Some preprocessing like scaling and centering was done over training data to reduce heterogeneity among texture and spectral data. Resampling was also conducted to prevent from over-fitting which is common in large cost values. The method used in resampling was 10-fold cross-validation with 5 time repetition. The tuning process was done over a grid search to find the optimum values of associated parameters. To this end, range of cost values were assigned between 2^{-2} and 2^7 and the corresponding sigma values was chosen on basis of the optimum cost value.

3.RESULTS AND DISCUSSION

This section presents the results of five different classification scenarios. Tuning over the defined grid at the first step was conducted for both scenarios and the results are presented in Table / Tablo 5. This table also contains columns regarding overall accuracy which produced from predicting over test samples and cross-validating accuracy associated with cross-validation over training samples.

Table 5. Different accuracy measures and optimum parameters in SVM method
Tablo 5. SVM metodunda farklı doğruluk ölçümleri ve optimum parametreler

Parameter Scenario	Optimum Cost Value	Optimum Sigma Value	Cross-validated accuracy	Overall accuracy
CNT method	64	0.382	0.845	0.8536
CNT & texture W3	32	0.154	0.855	0.8651
CNT & texture W5	32	0.143	0.891	0.8989
CNT & texture W7	128	0.145	0.91	0.9172
CNT & texture W9	64	0.161	0.929	0.9265

According to Table / Tablo 5, no specific trend was observed for optimum cost and sigma values. However, an incremental trend was discerned in both cross-validation and overall accuracy. The best results were yielded in case of addition of texture with window size 9 thereby the overall accuracy increased about 7%.

Further, to evaluate the performance of all scenarios, kappa coefficient, producer and user accuracy and conditional kappa are presented in Figure / Şekil 3, 4, 5 and Table / Tablo 6 and 7. P.A and U.A in Table / Tablo 6 denote producer accuracy and user accuracy respectively.

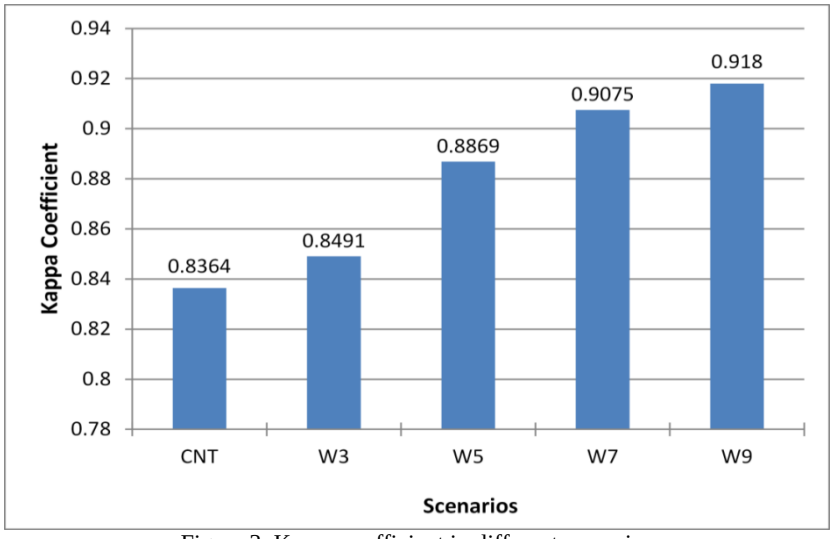

Figure 3. Kappa coefficient in different scenarios
Şekil 3. Farklı senaryolarda kappa katsayısı

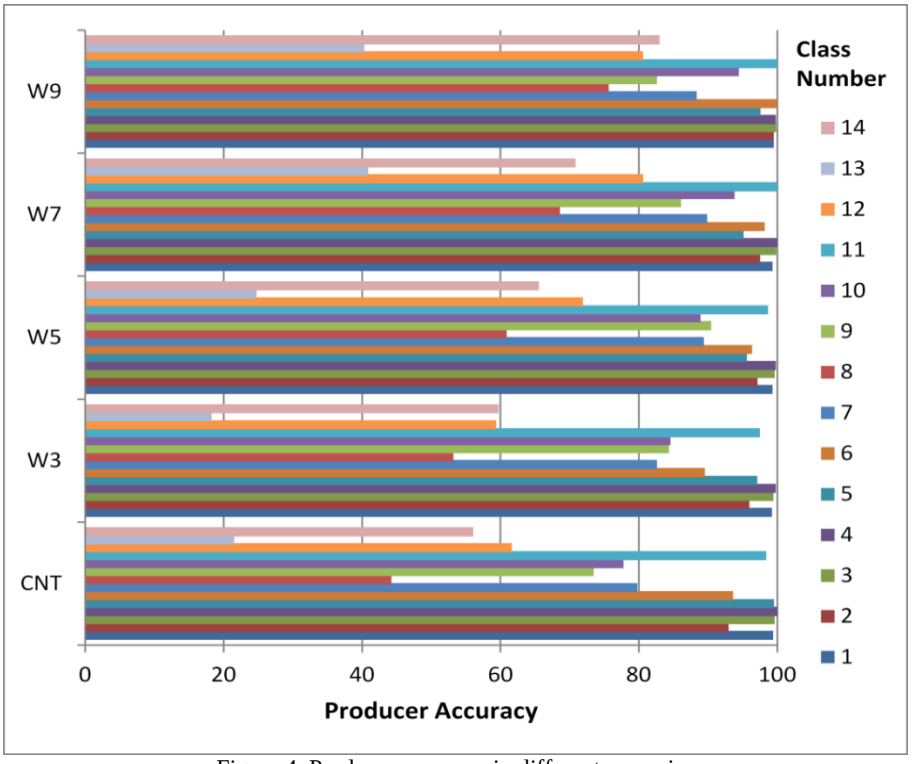

Figure 4. Producer accuracy in different scenarios
Şekil 4. Farklı senaryolarda üretici doğruluğu

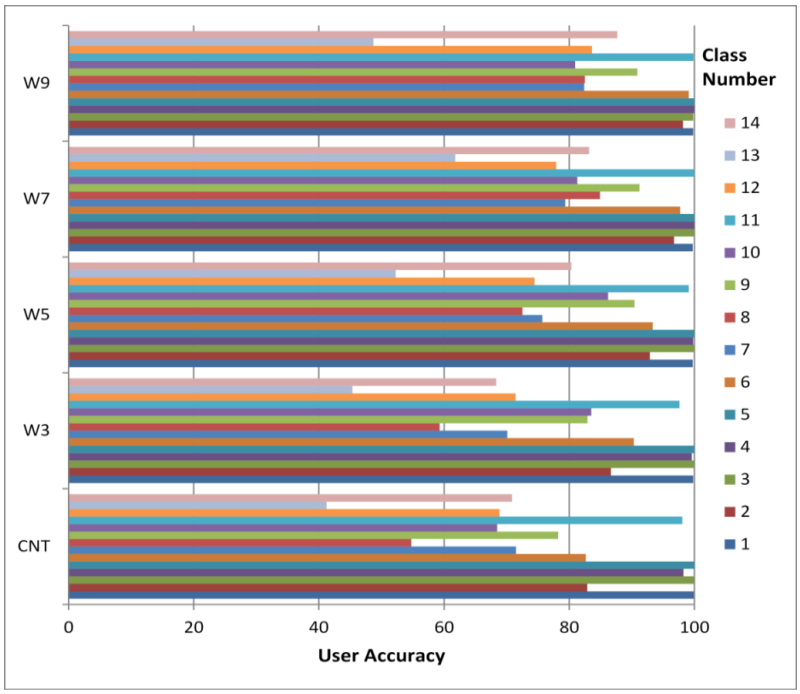

Figure 5. User accuracy in different scenarios
Şekil 4. Farklı senaryolarda kullanıcı doğruluğu

Table 6. Producer and user accuracy measures for different scenarios
Tablo 6. Farklı senaryolar için kullanıcı ve üretici doğruluğu ölçümleri

Scenario	**CNT**		**W3**		**W5**		**W7**		**W9**	
Class Number	**P.A**	**U.A**	**P.A**	**U.A**	**P.A**	**U.A**	**P.A**	**U.A**	**P.A**	**U.A**
1	99.39	99.91	99.21	99.82	99.3	99.74	99.3	99.74	99.48	99.82
2	92.95	82.89	95.95	86.67	97.13	92.88	97.52	96.76	99.48	98.2
3	99.62	100	99.44	100	99.62	100	99.81	100	99.81	99.81
4	100	98.25	99.8	99.8	99.8	99.80	100	100	99.8	100
5	99.51	100	97.09	100	95.63	100	95.15	100	97.57	100
6	93.61	82.66	89.5	90.32	96.35	93.36	98.17	97.73	100	99.1
7	79.77	71.49	85.59	70.11	89.4	75.7	89.88	79.38	88.33	82.4
8	44.23	54.76	53.21	59.29	60.9	72.52	68.59	84.92	75.64	82.52
9	73.48	78.24	84.35	82.91	90.43	90.43	86.09	91.24	82.61	90.91
10	77.78	68.48	84.57	83.54	88.89	86.23	93.83	81.28	94.44	80.95
11	98.38	98.09	97.5	97.64	98.68	99.11	100	100	100	99.85
12	61.64	68.88	59.36	71.43	71.92	74.47	80.59	77.92	80.59	83.65
13	21.52	41.24	18.28	45.33	24.73	52.28	40.86	61.79	40.32	48.7
14	56.07	70.86	59.71	68.33	65.53	80.36	70.87	83.19	83.01	87.69

The first scenario, i.e. classification based on CNT method has a satisfactory performance in class numbers between 1 to 6 in terms of both producer and user accuracy. These classes include different agricultural, barren lands and orchards. This can be justified in this way that the spectral data with high spectral resolution is sufficient for these land covers. Addition of texture derived from panchromatic image doesn't increase these classes accuracy substantially. This can be related to vast area covered with them and their homogenous texture compared to more complex land uses such as the residential and industrial areas in the region.

Comparison of producer and user accuracy values in Figure / Şekil 4 and 5 reveals the imbalance between these accuracy measures in different classes which is more evident in the residential and industrial areas.

High imbalance between producer and user accuracy exists mostly in warehouses, scattered and concentrated industries. The increase of window size in some classes such as warehouses and different types of industries reduces this imbalance which can be related to the role of texture for differentiating between these highly mixed areas. Conditional kappa measures can explain the overall effect of texture in variation of producer and user accuracy with a unique value thereby the analyzer can get a better idea of interaction of texture and spectral data. Table / Tablo 7 shows conditional kappa for all classes in all scenarios.

Table 7. Conditional kappa measure for different scenarios
Tablo 7. Farklı senaryolar için koşullu kappa ölçüsü

Scenario / **Class number**	**CNT**	**W3**	**W5**	**W7**	**W9**
1	0.9989	0.9979	0.9968	0.9968	0.9979
2	0.8067	0.8494	0.9196	0.9634	0.9796
3	1.0000	1.0000	1.0000	1.0000	0.9980
4	0.9811	0.9957	0.9979	1.0000	1.0000
5	1.0000	1.0000	1.0000	1.0000	1.0000
6	0.8207	0.8999	0.9314	0.9765	0.9906
7	0.6629	0.6466	0.7127	0.7562	0.7919
8	0.5368	0.5831	0.7186	0.8456	0.8210
9	0.7746	0.8230	0.9009	0.9093	0.9058
10	0.6769	0.8313	0.8588	0.8082	0.8048
11	0.9788	0.9738	0.9901	1.0000	0.9984
12	0.6669	0.6942	0.7267	0.7637	0.8250
13	0.3955	0.4376	0.5090	0.6069	0.4723
14	0.6894	0.6625	0.7906	0.8208	0.8688

CNT-based classification yields satisfactory conditional kappa coefficients values in classes 1 to 5. The only exception is class number 2, which relates to barren lands. This can be explained in a way that barren lands typically cover heterogeneous areas which can be treated by addition of texture. As it is evident in class 2, the addition of texture has increased conditional kappa coefficient from 0.8067 to 0.9796. The addition of texture with higher window sizes in other classes results in the increase of accuracy. However, in some classes such as roads, tree rows and warehouses, the best performance is achieved in window size 7. This can be related to the dependency of these classes to the boundary edges which is faded in high texture window size and explained in prior sections. Conditional kappa has the highest increase in the most heterogeneous classes such as warehouses, scattered and concentrated industries and residential areas (by about 50%) which confirms the role of texture in improvement of these highly mixed zones.

Warehouses had the lowest accuracy in this study which can be related to different factors: First, The mixed nature of these areas where contain several sub-covers such as stored construction materials, the asphalt pavement used in their courtyards. Second, the less area coverage compared to the other land covers such as barren lands and corn fields also make their differentiation from the other classes more complicated.

Finally, the classification map derived in CNT-based classification (a) and the ones which yielded from the addition of texture from window sizes 3, 5, 7 and 9 (b, c, d, e) is illustrated in figure 6. Some improvements such as the edge enhancement and omission of irrelevant pixels are discernable in the thematic maps generated by the addition of texture in different window sizes.

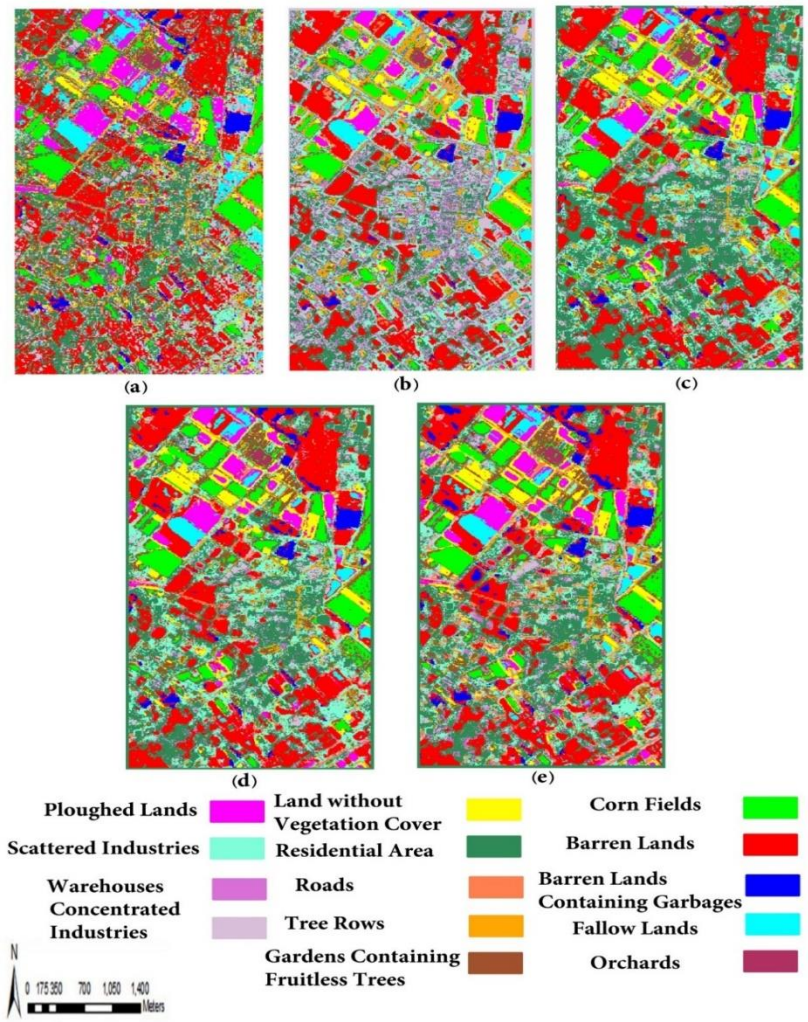

Figure 6. Thematic maps generated by all scenarios: a) the one generated by CNT method and b), c), d) and e) which generated by addition of texture with window sizes 3, 5, 7 and 9 respectively.
Şekil 6. Tüm senaryolar tarafından oluşturulan tematik (konusal) haritalar a) CNT metodu tarafından üretilen harita ve b), c), d) ve e) ise sırasıyla 3, 5, 7 ve 9 tekstür ölçülerine göre üretilen haritalardır.

Findings of this study were similar to Wang and Zhang (2014) who incorporated texture and NDVI as ancillary data for classification by SVM method. However, they used texture derived from the first and second PCs in principal component analysis. The use of Quickbird image with 0.62 m spatial resolution allowed them to evaluate the window sizes by even 41x41, but the coarser ALI panchromatic image spatial resolution limited our maximum window size to 9. The best classification performance in their study was achieved by incorporation of NDVI and texture to the spectra data which resulted in 30% increase in overall accuracy. However, addition of texture was the second best scenario which led to 23% increase in overall accuracy. Our study also gained 7% improvement of overall accuracy in case of addition of texture with window size 9 and substantial increase of heterogeneous areas such as industries which confirmed the hypothesis that addition of texture as an ancillary data improves the hyperspectral imagery classification.

4.CONCLUSION

This study investigated whether using texture information (i.e. GLCM) can improve the accuracy of urban classification within Hyperion satellite imagery. We explored several combinations of Hyperspectral and GLCM features in classifications of urban area with 14 numbers of different classes.

The classification results show that the urban areas of south west of Tehran are insufficiently characterized by the Hyperion satellite imagery. A quantitative assessment of the results, demonstrated that the use of texture information in urban land covers classification improved accuracy of classes with the high mixed pixels including tree rows, roads and residential areas considerably. So that, the overall accuracy increased by about 7% and some land use/ land covers such as residential and industrial areas and tree rows experienced to even 25% increase in classification accuracy.

Incorporation of the texture information, represented by the GLCM features, leads to a considerable decrease in the omission and commission errors. Accordingly, combining of texture information (i.e. GLCM) with Hyperion imagery decreases class confusion specifically in heterogonous classes. The GLCM features show great potential for land use cover classification in heterogeneous areas with rich textural information (e.g. urban area). Meanwhile, the accuracy of classification using texture measures depends highly on the window size which efficiently investigated in this study.

In the end, the evaluation of other fusion methods such as principal component transformation, naïve bayes are proposed for future studies. The addition of different ancillary data with higher spatial resolution such as IKONOS, RADAR and so on is also recommended.

ACKNOWLEDGEMENT (TEŞEKKÜR)

The authors wish to thank U.S. Geological Survey (USGS) for providing us with Hyperion and ALI images through online services. We also want to thank Mr. Mohammad Sedghi for constructive reviews and linguistic modifications on the primary manuscript. Finally, we would like to thank anonymous referees who provided valuable feedbacks on earlier version of this paper.

REFERENCES (KAYNAKLAR)

Bokoye, A.I., Dionne, P., 2004. Urban material characterization from the Hyperion hyperspectral imager: Application to downtown Montreal (Quebec, Canada). *Image and Signal Processing for Remote Sensing* 5238: 569- 574. Conference No.9, Barcelona, Spain, Doi: http://dx.doi.org/10.1117/12.511150

Camps-Valls, G., Bruzzone, L., 2005. Kernel-based methods for Hyperspectral image classification, *IEEE Transactions on Geoscience Remote Sensing* 43: 1351–1362.

Carleer, A. P., Wolff, E, 2006. Urban land covermulti-level region-based classification of VHR data by selecting relevant features. *International Journal of Remote Sensing* 27: 1035−1051.

Carlson, T.N., Sanchez-Azofeifa, G.A. 1999. Satellite remote sensing of land use changes in and around San José, Costa Rica. *Remote Sensing of Environment 70*: 247–256.

Cavalli, M.R., Fusilli, L., Pascucci, S., Pignatti, S., Federico Santini, F., 2008. Hyperspectral Sensor Data Capability for Retrieving Complex Urban Land Cover in Comparison with Multispectral Data: Venice City Case Study (Italy). *Sensors* 8: 3299-3320. Doi: http://dx.doi.org/10.3390/s8053299

Clausi, D. A., Yue, B., 2004. Comparing co-occurrence probabilities and Markov random fields for texture analysis of SAR sea ice imagery. *IEEE Transaction on Geoscience and Remote Sensing* 42: 215-228.

Colgan, M. S., Baldeck, C. A., Féret, J. B., Asner, G. P., 2012. Mapping savanna tree species at ecosystem scales using support vector machine classification and BRDF correction on airborne hyperspectral and LiDAR data". *Remote Sensing* 4(11): 3462-3480. Doi: http://dx.doi.org/10.3390/rs4113462

Féret, J., Asner, G. P., 2013. Tree species discrimination in tropical forests using airborne imaging spectroscopy. *IEEE Transactions on Geoscience Remote Sensing* 51: 73-84.

Forster, B.C., 1985. An examination of some problems and solutions in monitoring urban areas from satellite platforms. *International Journal of Remote Sensing* 6: 139-151. Doi: http://dx.doi.org/10.1080/01431168508948430

Fauvel, M., 2007. Spectral and spatial methods for the classification of urban remote sensing data, Ph.D. dissertation, Grenoble Inst. Technol., Grenoble, France.

Fauvel, M., Benediktsson, J.A., Chanussot, J., Sveinsson, J.R., 2008. Spectral and Spatial Classification of Hyperspectral Data Using SVMs and Morphological Profiles. *IEEE Transactions on Geoscience Remote Sensing* 46: 3804-3814. Doi: http://dx.doi.org/10.1109/TGRS.2008.922034

Goetz, A.F.H., 2009. Three decades of hyperspectral remote sensing of the Earth: A personal view. *Remote Sensing of Environment* 113: S5–S16. Doi: http://dx.doi.org/10.1016/j.rse.2007.12.014

Goumehei, E., 2010. Contextual image classification with support vector machine". M.Sc Thesis, ITC, Enscede.

Gualtieri, J.A., 2009. The Support Vector Machine (SVM) algorithm for supervised classification of hyperspectral remote sensing data, In: Kernel Methods for Remote Sensing Data Analysis, Edited by Camps-Valls, G., & Bruzzone, L., Wiley, New York, 51-83.

Hall-Beyer, M., 2007. GLCM Texture: A Tutorial, Version 2.10. Viewed 16 http://www.fp.ucalgary.ca/mhallbey/tutorial.htm.

Haralick, R.M., 1979. Statistical and structural approaches to texture. *In: Proceedings of the IEEE* 67: 786–804.

Haralick, R.M., Shanmugam, K., Dinstein, I., 1973. Textural features for image classification. *IEEE Transactions on Systems* Man, and Cybernetics SMC-3 610–621 November (6).

Huang, C., Davis, L.S., Townshend, J.R.G., 2002. An assessment of support vector machines for land cover classification". *International Journal of Remote Sensing* 23: 725-749. Doi: http://dx.doi.org/10.1080/01431160110040323

Kawishwar. P., 2007. Atmosphere correction models for retrievals of calibrated spectral profiles from Hyperion EO-1 data, M.Sc. Thesis, ITC, Enscede.

Mather, P., Tso, B., 2009. Classification methods for remotely sensed data (Second Edition). CRC press. Boca Raton.

Melgan, F., Bruzzone, L., 2004. Classification of hyperspectral remote sensing images with support vector machine, *IEEE Transactions on Geoscience and Remote Sensing* 42: 1778-1790. Doi: http://dx.doi.org/10.1109/TGRS.2004.831865

Mountrakis, G., Im, J., Ogole, C., 2011. Support vector machines in remote sensing: A review. *ISPRS Journal of Photogrammetry and Remote Sensing* 66: 247-259. Doi: http://dx.doi.org/10.1016/j.isprsjprs.2010.11.001

Murray, H., Lucieer, A., Williams, R., 2010. Texture-based classification of sub-Antarctic vegetation communities on Heard Island. *International Journal of Applied Earth Observation and Geoinformation* 12: 138- 149. Doi: http://dx.doi.org/10.1016/j.jag.2010.01.006

Oommen, T., Misra, D., Twarakavi, N. K., Prakash, A., Sahoo, B., Bandopadhyay, S., 2008. An objective analysis of support vector machine based classification for remote sensing. *Mathematical Geosciences* 40: 409-424. Doi: http://dx.doi.org/10.1007/s11004-008-9156-6

Pacifici, F., Chini, M., Emery, W.J., 2009. A neural network approach using multi-scale textural metrics from very high-resolution panchromatic. *Remote Sensing of Environment* 113: 1276–1292.

Pacifici, F., Del Frate, F., Solimini, C., Emery, W.J. 2007. An innovative neural-net method to detect temporal changes in high-resolution optical satellite imagery. *IEEE Transaction on Geoscience and Remote Sensing* 45: 2940−2952.

Petropoulos, G.P., Knorr, W., Scholze, M., Boschetti, L., Karantounias, G., 2010. Combining ASTER multispectral imagery analysis and support vector machines for rapid and cost-effective post-fire assessment: a case study from the Greek wildland fires of 2007. *Natural Hazards and Earth System Science* 10: 305-317. Doi: http://dx.doi.org/10.5194/nhess-10-305-2010

Puissant, A., Hirsch, J., &Weber, C. (2005). The utility of texture analysis to improve perpixel classification for high to very high spatial resolution imagery. *International Journal of Remote Sensing* 26: 733−745.

Ridd, M.K. 1995. Exploring a V–I–S (vegetation–impervious surface–soil) model for urban ecosystem analysis through remote sensing: comparative anatomy for cities. *International Journal of Remote Sensing* 16: 2165-2185.

Shanmugan, K. S., Narayanan, V., Frost, V. S., Stiles, J. A., Holtzman, J. C., 1981. Textural features for Dadar image analysis. *IEEE Transactions on Geoscience and Remote Sensing* 19: 153−156.

Small, C. Scaling Properties of Urban Reflectance Spectra. *In Proceeding of AVIRIS Earth Science and Applications Workshop,* Pasadena, CA, 27 Feb -2 Mar, 2001.

Small, C., 2005. A global analysis of urban reflectance. *International Journal of Remote Sensing* 26: 661-681. Doi: http://dx.doi.org/10.1080/01431160310001654950

Wang, L., Zhang, S., 2014. Incorporation of texture information in a SVM method for classifying salt cedar in western China. *Remote Sensing Letters* 5: 501-510. Doi: http://dx.doi.org/10.1080/2150704X.2014.928422

Welikanna, D.R., Tolpekin, V., Yogesh K., 2008. Analysis of the Effectiveness of Spectral Mixture Analysis and Markov Random Field Based Super Resolution Mapping Over an Urban Environment. *The International Archives of the Photogrammetry, Remote Sensing and Spatial Information Science* Vol XXXVII, Part B7: 641-649

Yuntao, Q., Minchao, Y., Jun, Z., 2012. Hyperspectral Image Classification Based on Structured Sparse Logistic Regression and Three-Dimensional Wavelet Texture Features. *IEEE Transactions on Geoscience Remote Sensing* 51: 2276-2291.

Zhang, Q.,Wang, J., Gong, P., Shi, P., 2003. Study of urban spatial patterns from SPOT panchromatic imagery using textural analysis. *International Journal of Remote Sensing* 24: 4137-4160. Doi: http://dx.doi.org/10.1080/0143116031000070445